

Development of a Feed-Forward Compensation Technique to Calculate Beam Position in the Mitigation of Platform-Induced Jitter

Matthew Roberts, Joe Watkins,* and Oscar Barton, Jr.

Mechanical Engineering Department, U.S. Naval Academy, Annapolis, Maryland 21402

Beam control is essential for the development and operation of a directed energy system, especially when operating in the air or on the sea in a combat maritime environment. Directed energy beams are susceptible to jitter due to platform-induced vibrations and atmospheric effects. To correct jitter caused by mechanical vibrations without feedback from the target, the exact position and orientation of the platform must be determined in real time. A unique laser jitter control test bed is used to develop the necessary algorithms and sensor placements that are suitable for calculating the platform-induced error in the directed energy beam in real time. This error can then be used in a feed-forward compensation technique to calculate the beam position that mitigates platform-induced jitter. The paper introduces the algorithm and initial results in predicting jitter for a complex pitch motion using a least-mean-squares adaptive filter.

KEYWORDS: Directed energy, Feed forward, Jitter, LMS filter

Nomenclature

d	distance along a beam direction to the intercept plane
m_{ij}	i th component of the j th coordinate on the intercept plane
n_i	i th component of the direction of the normal to a plane
\mathbf{r}	direction vector
$[T_{\text{ref}}]$	reflection matrix
$[T_{\text{rot}}]$	rotation matrix
$\bar{w}_m(n)$	vector of length m of weights at discrete step n
\bar{x}	intercept point of a vector
$y(n)$	output at step n
$\varepsilon(n)$	prediction error at step n
μ	least-mean-squares filter adaptation rate
$v(n)$	zero mean white noise process of variance σ_v^2

Received February 25, 2010; revision received May 7, 2010.

*Corresponding author; e-mail: rwatkins@usna.edu.

1. Introduction

The first efforts to remove disturbances from unwanted vibrations in optical beams were in overcoming the problem of image stabilization. Smith¹⁰ wrote one of the first papers, published in 1928, on the algebraic theory behind systems of plane reflecting surfaces. Beggs¹ developed an algorithm in 1960 for quantifying mirror-image kinematics. Both of these methods used matrix algebra to solve the image location on a focal plane for a series of reflections. In 1990, Royalty⁷ applied these matrix techniques to a gimballed mirror in anticipation of using these systems on vehicles that could impart motion to the mirror itself. DeBruin and Johnson² applied vector analysis to establish a line-of-sight reference frame, again for a mirror disturbed by motion of the base. In-depth research into the control of optical beams first began in the 1980s and 1990s for use in satellite communications,⁹ and adaptive control has been proposed for use in control systems for accurate beam pointing.⁸ The use of directed energy beams as weapons was explored during this time, but laser systems and power requirements were too large, making them impractical for naval applications. The recent advent of smaller lasers with high power output has prompted the Navy to explore the use of directed energy systems on tactical naval platforms. For the Navy to move forward with a directed energy system, beam control technology must be advanced to minimize the power-dissipating effects of jitter.

In the 1990s, the Air Force began work on a high-altitude directed energy system that had the potential to shoot down theater ballistic missiles.³ Currently several ground-based directed energy programs are in development as well. These systems have demonstrated the ability to detect, track, and destroy targets, but they do not experience the dynamics of a tactical naval platform and are therefore not subject to the higher amplitude mechanical vibrations expected to be encountered in a combat maritime environment. More important, the dynamic nature of the maritime and/or low-altitude combat environment may make obtaining accurate feedback of the beam's location on the target problematic. Therefore, a jitter mitigation technique that uses a feed-forward error signal, as opposed to feedback, is desirable. Orzechowski et al.⁶ discussed an adaptive system in which the statistics of the disturbance are fed forward, but the error signal is developed using feedback from the beam position. Sofka et al.¹¹ use feed-forward inertial position to stabilize a positioning system (the Omni-Wrist III), but incorporated feedback of an optical detector to produce the position error signal. Skormin⁹ developed a self-tuning regulator and also used model reference control⁸ to feed forward the fast steering mirror (FSM) structural dynamics and platform motion. These systems developed feed-forward compensation techniques to aid in jitter control but still utilized feedback from a detector to determine the beam position error signal.

The following technique develops an algorithm to compute the beam's motion based on the platform's motion and mirror kinematics alone with no reference to the target for jitter control. Although previously unavailable, today's faster CPUs and I/O cards present an opportunity to exploit extraordinarily sensitive rate and acceleration sensors to determine the platform's motion. High computational power may also allow for the combination of the beam's calculated motion with adaptive filters to predict the beam's position for use as an error signal in control systems. Combined, this research has the potential to improve the aim point maintenance on a target, thus significantly reducing the power required for a directed energy system. However, prior to being used in an actual system, transition to an on-board and line-of-sight reference system instead of the external reference presented here must be made and will be attempted in future planned work. This paper is organized

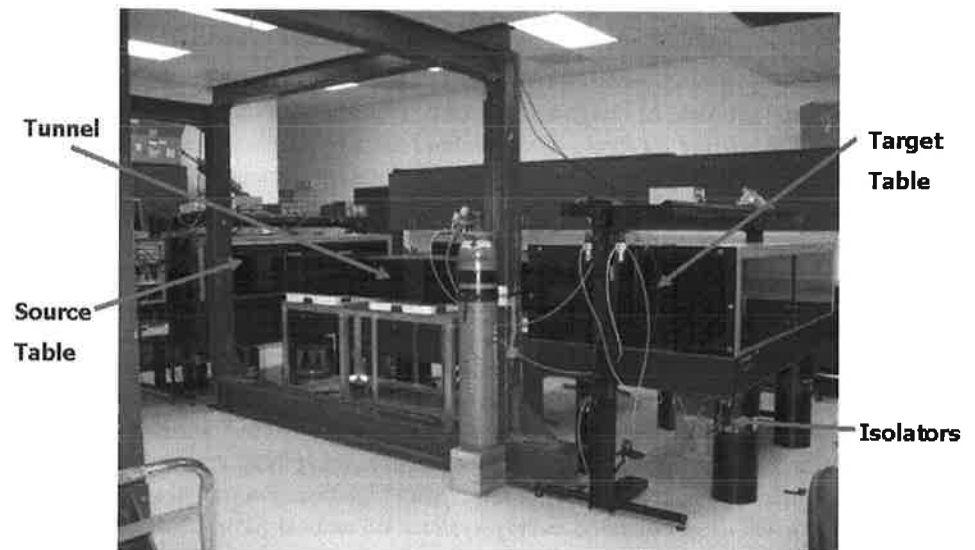


Fig. 1. USNA directed energy control laboratory.

as follows: first, a discussion of the experimental setup; following that, the theory used to develop the feed-forward signal will be explained; and finally, experimental results and conclusions will be presented.

2. Experimental Setup

2.1. Description of major components

Research for this project was conducted in the U.S. Naval Academy (USNA) Directed Energy Control Laboratory, as seen in Fig. 1.

The Newport Corporation's FSMs are the heart of the beam control system as they are used to rapidly and accurately direct the beam through the system. The FSMs use voice coils to position the mirrors in response to commanded inputs. The FSMs have a control bandwidth ranging from about 300 to 1,000 Hz, depending on the size of the mirror used. A Newport research-grade breadboard with constrained layer damping simulates the directed energy beam's source platform. It is a $36 \times 36 \times 2$ in. honeycombed breadboard constructed to eliminate torsional and bending modes below about 200 Hz. The breadboard is mounted on a Newport research-grade optical table using four compression springs and four isolators. Simulation of the vibrations that would be encountered on an aircraft will be accomplished by inertial actuators. These actuators are configured in such a way as to impart multiple-frequency periodic motion as well as random vibrations to the platform.

To determine the position and orientation of the platform as well as the beam's position on target, On-Trak's position-sensing detectors (PSD) and mountings [designated a position-sensing module (PSM)] are driven by an On-Trak OT301 position-sensing amplifier. The combination is used to measure the movement of the main beam and positioning beams. The PSMs have a detection area of 10×10 mm and provide the position of the center of

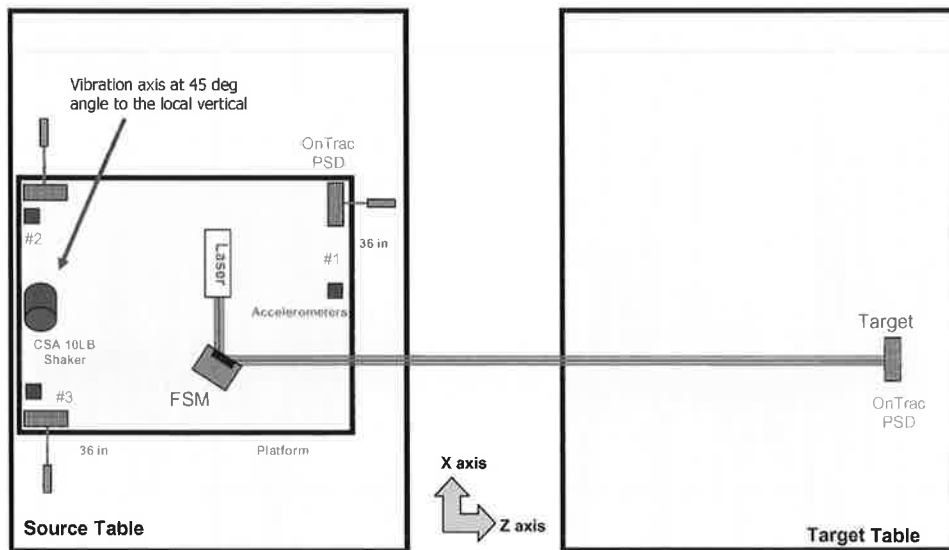


Fig. 2. Experimental configuration. Total laser distance: 5 m from exit aperture on platform to target.

the laser beam in two dimensions. The minimum resolution of the PSM is approximately $0.5 \mu\text{m}$ when combined with the OT301 amplifier. The lasers used on the platform and for the main beam are 5-mW, 635-nm diode lasers, with an elliptical beam measuring $3.8 \times 0.9 \text{ mm}$. The main beam is circularized by an anamorphic prism pair.

The computer control system is based on MATLAB R2006b with SIMULINK from Mathworks and the xPC Targetbox from SpeedGoat. The main computer for control implementation and experiment supervision is a Dell Precision 690 workstation with a CPU speed of 3.8 GHz. The xPC Targetbox is an Intel Core 2 Duo running at 2.13 GHz.

2.2. Experimental method

This research project uses the configuration in Fig. 2 to calculate an error signal by determining the position and orientation in real time for the full beam control system. The configuration contains the platform, one inertial actuator mounted at a 45-deg angle to the platform's surface, four PSMs, and the laser. Three "position" PSMs are on the platform, with a diode laser mounted next to them off the platform, to develop the position of three points on the surface. The position PSMs will move with the platform, and their associated diode laser will remain fixed on the optical table. The motion of the position PSMs translates into an x - y laser position on each PSM's detection area. Assuming that the positions of the PSMs do not change, the known distance between the position PSMs can be used to find the equation of the plane. The fourth PSM will be the target, approximately 5 m away. It is recognized that this type of measurement system cannot be used on a mobile platform. However, if an error signal can be developed that is suitable for correcting the beam, the calculated beam error as a function of accuracy in the position and orientation may be known. The specifications for an on-board inertial measurement unit (IMU) may then be determined to accomplish the desired accuracy for the error signal.

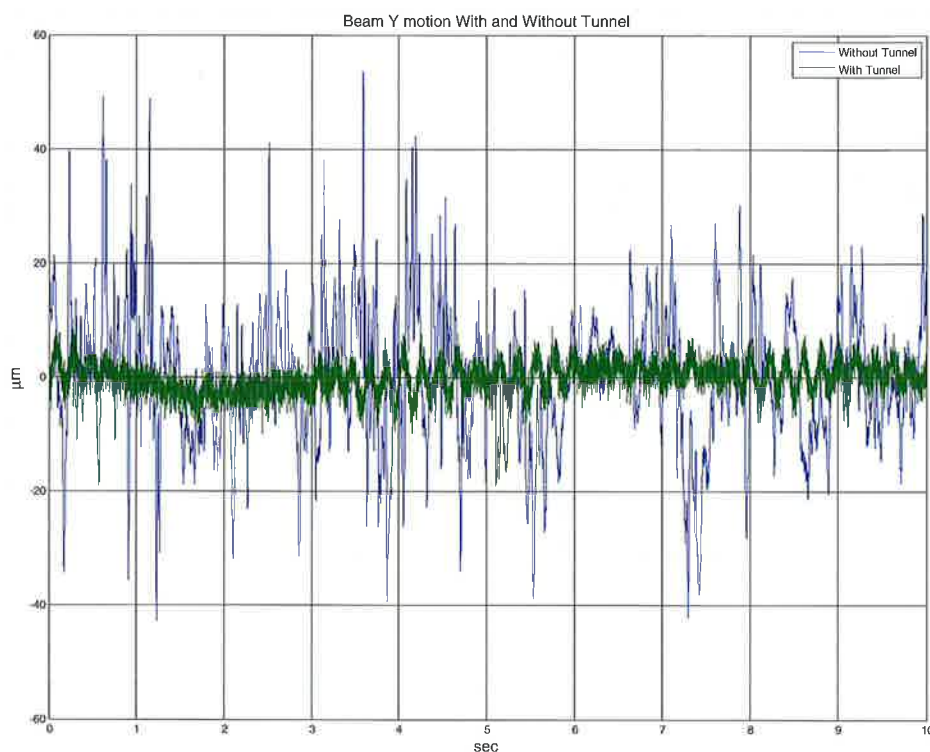


Fig. 3. Tunnel effects.

In the experiment, the platform is disturbed by the inertial actuator using multiple frequencies along with random noise. The positions of three points on the platform, in two dimensions at each point, are measured using the position PSMs in a time step of 1 ms as the platform is disturbed by the inertial actuator. These measurements are used to generate an algorithm to determine the position and orientation of the platform as a function of time. Knowing this motion and each reflective surface's orientation, the beam intercept point is then calculated and compared to the laser motion at the target.

2.3. Tunnel isolation effects on jitter

The entire laboratory setup is enclosed by acrylic windows in an effort to mitigate possible atmospheric or acoustic disturbances. After the beam is reflected off the FSM, it travels through a tunnel approximately 5 m before it intercepts the target PSM. Figure 3 shows the effects of the tunnel on the beam's vertical position at the target. For this experiment, the platform was not disturbed and the FSM was held at a fixed position. Figure 3 shows that the jitter is noticeably reduced, and the transverse motion of the platform due to acoustic and seismic disturbances within the laboratory is clearly seen. This setup will allow experimental verification that the platform-induced jitter has been mitigated

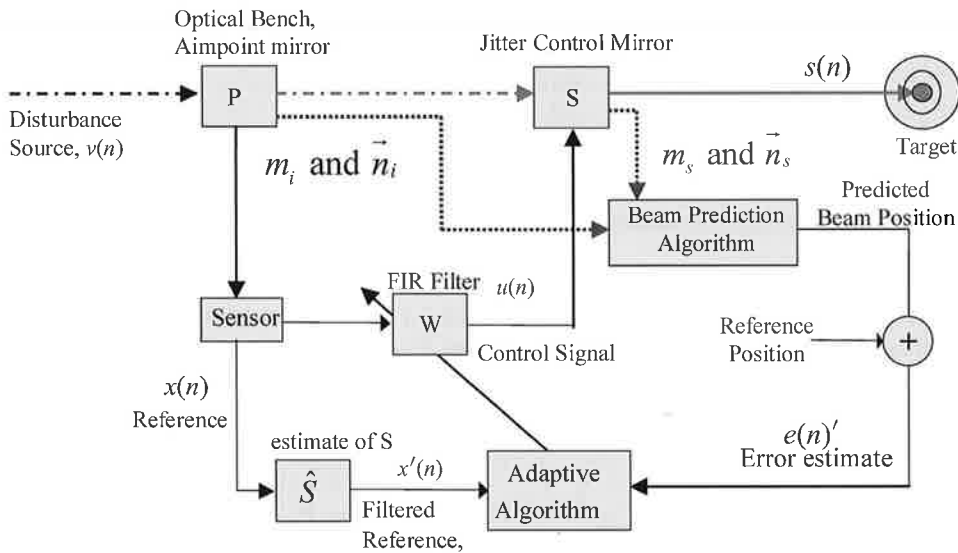


Fig. 4. Adaptive control model block diagram: open loop.

3. Theory

3.1. Calculated beam position

To correct platform-induced jitter, the error between the beam's actual impact and its intended impact point must be determined. This is normally accomplished by using feedback from the target. Obtaining feedback may be problematic in the expected environment. Therefore a feed-forward control system is proposed to mitigate the jitter imposed by the platform. A feed-forward system will require the beam's path to be predicted in real time. Applying rigid body kinematics for the platform and the laws of geometric optics to the optical control system provides the means of determining the position of the impact of the beam at the target based only on platform motion. Atmospheric effects may be corrected by other means such as deformable mirrors and probe beams. Assuming that the platform on which the beam source and control mirrors are mounted is rigid, the position and orientation of the platform, and any point on it, can be determined, given accurate sensory input. The platform used in the experimental apparatus rests atop four springs that allow limited displacement and rotation in six degrees of freedom. From sensors, the position of the platform at three points can be measured, and using these three points the equation for the platform's surface can be determined. This equation can be used to find the displacement and orientation of the composite bodies on the platform, specifically the starting location of the beam and the orientation of the reflective surfaces that controls the beam. From this information, the plane for each reflective surface may be determined. Geometric optics can be introduced to predict where the beam will travel given the orientation of its source and the reflective surfaces that control it. In addition to the orientation of the reflective surfaces on the platform, the mirrors can rotate about two axes to control the beam's direction. The rotation of the mirror is reported by the mirror's sensing system, which provides the necessary information required to compute the normal vector to each reflective surface.

The normal is then used to generate a reflection matrix, $[T_{\text{ref}}]$:

$$[T_{\text{ref}}] = \begin{bmatrix} 1 - 2n_1^2 & -2n_1n_2 & -2n_1n_3 \\ -2n_1n_2 & 1 - 2n_2^2 & -2n_2n_3 \\ -2n_1n_3 & -2n_2n_3 & 1 - 2n_3^2 \end{bmatrix}, \quad (1)$$

where n_i is the i th component of the vector normal to the plane calculated from the mirror and platform position and orientation. The original direction of the beam, \mathbf{r} , is multiplied by this reflection matrix to determine the new direction of the beam, \mathbf{r}' :

$$\mathbf{r}' = [T_{\text{ref}}]\mathbf{r}. \quad (2)$$

This new direction, along with the starting point \bar{x} and distance to the next point (d), is used to determine the intercept point of the beam \bar{x}' on the next intercept plane:

$$\bar{x}' = \bar{x} + \bar{r} d. \quad (3)$$

d is calculated as

$$d = \frac{\det \begin{bmatrix} 1 & 1 & 1 & 1 \\ m_{1,1} & m_{2,1} & m_{3,1} & x_1 \\ m_{1,2} & m_{2,2} & m_{3,2} & x_2 \\ m_{1,3} & m_{2,3} & m_{3,3} & x_3 \end{bmatrix}}{\det \begin{bmatrix} 1 & 1 & 1 & 0 \\ m_{1,1} & m_{2,1} & m_{3,1} & r_1 \\ m_{1,2} & m_{2,2} & m_{3,2} & r_2 \\ m_{1,3} & m_{2,3} & m_{3,3} & r_3 \end{bmatrix}}, \quad (4)$$

where the $m_{i,j}$ are the i th component of the j th coordinate on the intercept plane. Three arbitrary points on the intercept plane (the $m_{i,j}$) are required to find the intercept point.

The intercept point and the beam direction from the last reflective surface on the platform are determined in the platform coordinate system. To find the point in the target's coordinate system, the last reflective surface's intercept point and beam direction are multiplied by a rotation matrix, $[T_{\text{rot}}]$:

$$[T_{\text{rot}}] = \begin{bmatrix} c(\Delta y)c(\Delta z) & c(\Delta y)s(\Delta z) & -s(\Delta y) \\ s(\Delta x)s(\Delta y)c(\Delta z) - c(\Delta x)s(\Delta z) & s(\Delta x)s(\Delta y)s(\Delta z) + c(\Delta x)c(\Delta z) & s(\Delta x)c(\Delta y) \\ c(\Delta x)s(\Delta y)c(\Delta z) + s(\Delta x)c(\Delta z) & c(\Delta x)s(\Delta y)s(\Delta z) - s(\Delta x)c(\Delta z) & c(\Delta x)c(\Delta y) \end{bmatrix}. \quad (5)$$

The c and s signify cosine and sine of the angle, respectively. The angle is the angle about the pitch (Δx), roll (Δz), and yaw (Δy) axes, with the roll axis being the axis in the direction of the target. The position and the beam direction in the target frame of reference is then found by

$$\bar{x}_I = [T_{\text{rot}}]\bar{x}_P, \quad (6)$$

$$\mathbf{r}_I = [T_{\text{rot}}]\mathbf{r}_P. \quad (7)$$

The subscript I indicates the target frame of the reference coordinate system (inertial coordinate system in the case of the laboratory setup). The values of the intercept point *on* the last plane and the direction *from* the last plane must be in the target frame of reference and used in the calculation of d for the distance to the target in Eq. (4).

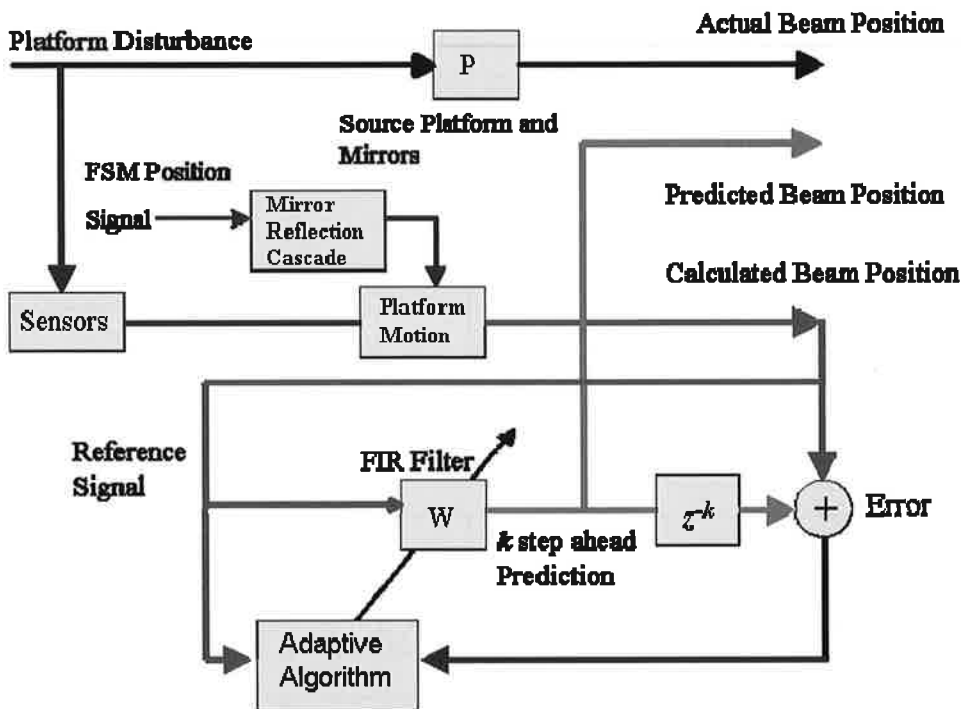


Fig. 5. Block diagram of beam prediction algorithm.

For the case of multiple mirrors, if the intercept point is another reflective surface, this process is repeated using the next mirror orientation, the intercept point on the previous mirror, the beam direction after reflection, and the distance d as calculated by Eq. (4). For multiple reflective surfaces, the following algorithm may be used:

$$\bar{x}_I = [T_{\text{rot}}] \left\{ {}^o x_P + \sum_{i=0}^k \left(\prod_{j=0}^i [T_{\text{ref}}^j] \right) {}^o r_P^{i+1} d \right\}, \quad (8)$$

where k is the number of reflective surfaces, ${}^0[T_{\text{ref}}] = [I]$ (identity matrix), ${}^k d$ is in the target's frame of reference, and ${}^j[T_{\text{ref}}]$ is the reflection matrix for the j th mirror.

If this intercept point is the target, then the impact position is theoretically known and the error can be determined. This error can then be used in a feed-forward compensation technique using adaptive filters to predict the beam's position

3.2. Beam prediction

In an adaptive control architecture, the error between the desired position and the actual must be provided to the algorithm (Fig. 4).

Using the calculation described in Sec. 2.1, a method can be determined for providing this error. However, this calculation will always be time late. The jitter control mirror will be positioned based on the error at the current time minus the calculation interval, but by the time the command is generated and the mirror moved, the platform may have changed position enough to affect the platform-induced jitter appreciably. To overcome the time-late beam correction, a beam prediction scheme is proposed.

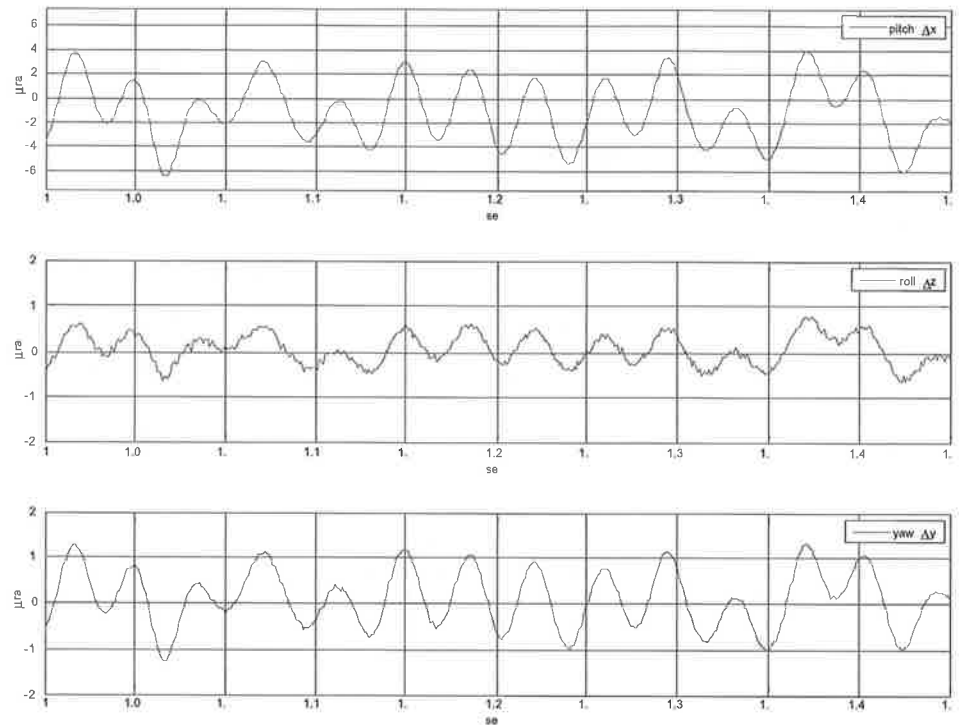


Fig. 6. Platform motion.

By using a k step-ahead prediction algorithm, the beam's position at a time k steps ahead may be determined. As a first step in determining the validity of this approach and more important, the computational time needed to calculate a prediction, a simple least-means-squares (LMS) single-step predictor is used. The LMS predictor provides an output at time t based on the outputs at time $t - 1$ and therefore does not predict into the future but "predicts" the current output. The k in Fig. 5 is zero for a single-step prediction of the current output.

The LMS predictor may be described as follows: For an autoregressive process of order m , the output $y(n)$ is

$$y(n) = \bar{w}_m(n)' \bar{y}_m(n-1) + v(n), \quad (9)$$

where $\bar{w}_m(n)$ is a vector of length m of weights at discrete step n (corresponding to time step t), $\bar{y}_m(n-1)$ is a vector of length m of outputs at $n-1$, and $v(n)$ is a zero mean white noise process of variance σ_v^2 . The $()'$ indicates transposition. For the LMS adaptive predictor,⁵ the weights are updated by

$$\hat{w}_m(n+1) = \hat{w}_m(n) + \mu \bar{y}_m(n-1) \varepsilon(n), \quad (10)$$

where the caret indicates an estimate, μ is the adaptation rate, and the prediction error $\varepsilon(n)$ is found by

$$\varepsilon(n) = y(n) - \hat{w}_m(n)' \bar{y}_m(n-1). \quad (11)$$

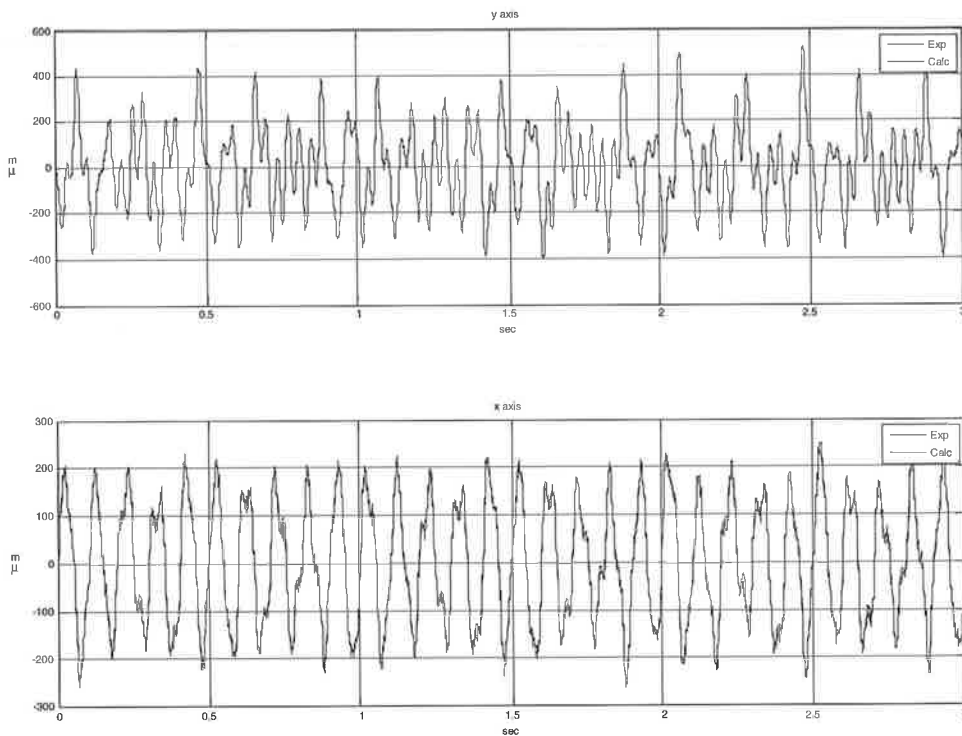


Fig. 7. Beam position and calculation at target.

The output of the predictor is then

$$\hat{y}(n) = \hat{w}_m(n)' \bar{y}_m(n-1). \quad (12)$$

4. Experimental Results

The experiment was conducted using one inertial actuator that imparted a complex pitch and yaw motion to the platform as it is mounted at a 45-deg angle to the horizontal axis of the platform. The rotation of the platform about the pitch, roll, and yaw axes in microradians is shown in Fig. 6. At the target, the position of the beam in the target coordinate system's y axis (vertical, top graph) and x axis (horizontal, bottom graph) is plotted in micrometers in Fig. 7. The average error between the actual and calculated jitter angle using the algorithm in Sec. 3.1 is shown in Fig. 8. The data in Fig. 8 were smoothed using a 50-ms moving average filter in order that the structure in the motion could be ascertained. As can be seen, the calculation is accurate within about $1 \mu\text{rad}$ using this moving average.

Figure 9 shows the actual beam position at the target in the target coordinate system's y axis (vertical, top graph) and x axis (horizontal, bottom graph) in micrometers. The predicted beam position at the target is also plotted on the same graph, showing the agreement between actual and predicted. Figure 10 illustrates the difference between the actual and predicted jitter angles at the target over the last 0.5-s span of the 3-s experiment.

This prediction was not expected to be that accurate, as it was a simple LMS filter. It is anticipated that a more accurate prediction can be made by using a self-tuning predictor¹² or a lattice-type predictor.⁴

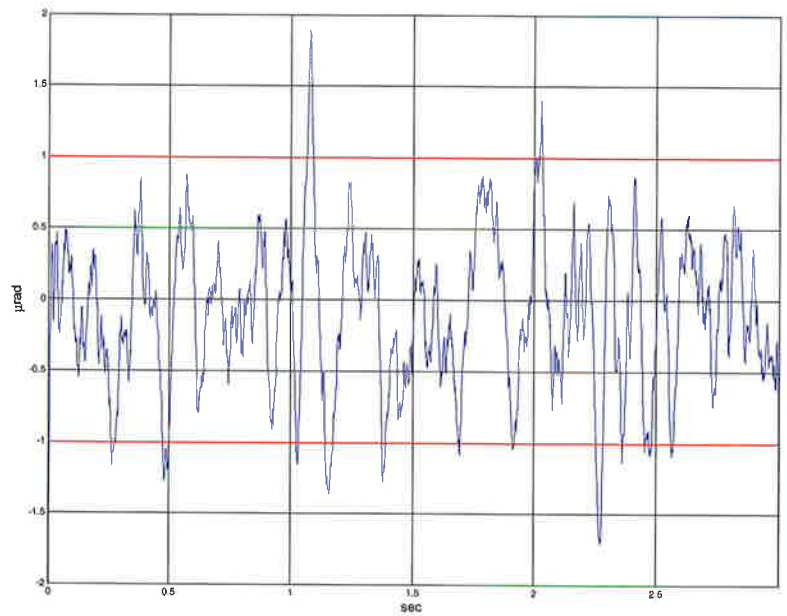


Fig. 8. 50-ms moving average between calculated and actual jitter angle.

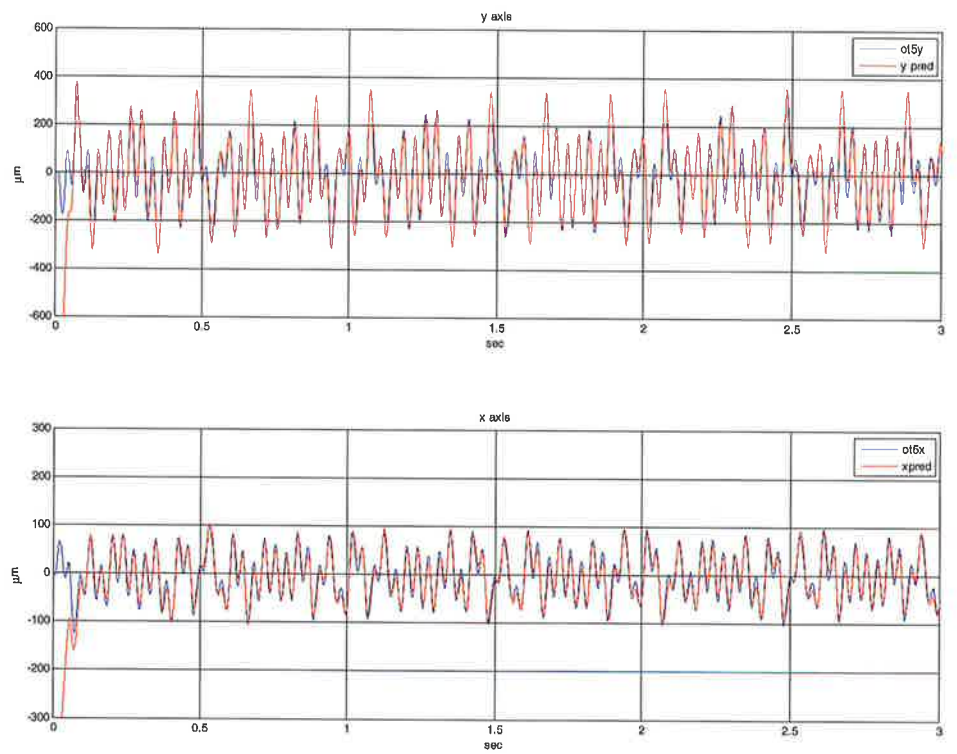


Fig. 9. Beam position and prediction at target.

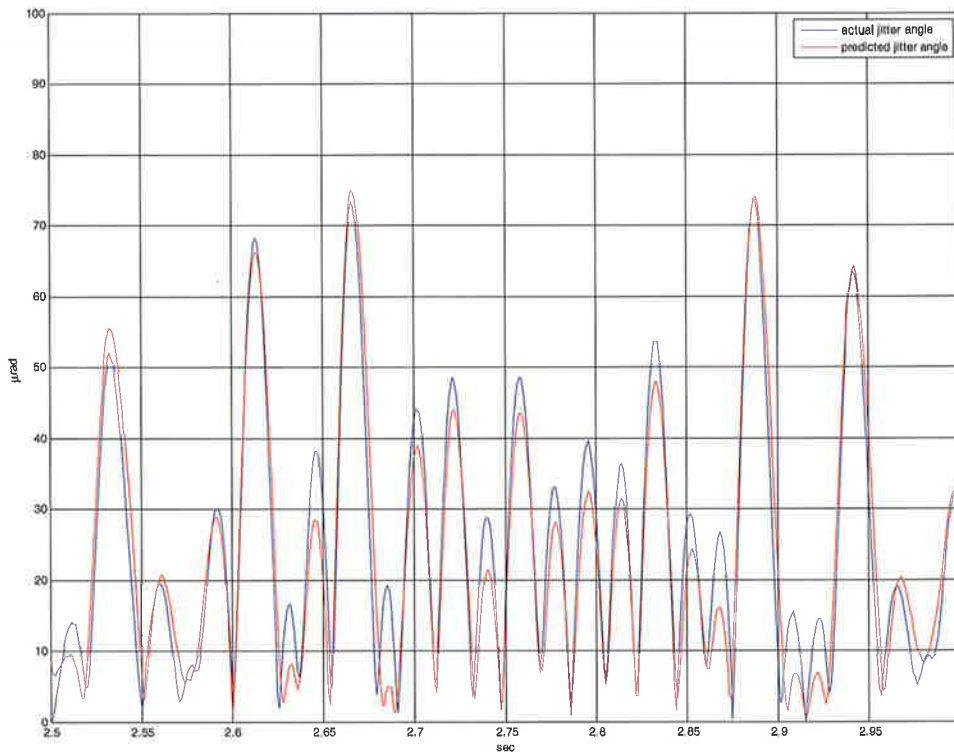


Fig. 10. Actual and predicted jitter angle.

5. Conclusions

This experiment demonstrates that it is possible to calculate the beam's position for a complex pitch and yaw motion based solely on the platform position and mirror angles in near real time. The calculated error had an RMS value of $1.88 \mu\text{rad}$ and was outside of a $\pm 1\text{-}\mu\text{rad}$ band for 0.2 s of a 3-s experiment using a 50-ms moving average. Using a one-step-ahead LMS prediction algorithm, this calculated position was used to predict the beam's position at the target at the current time. The sample time for the experiment was 1 ms. The maximum execution time, including the predictive algorithm, was only $40 \mu\text{s}$. Sample times of $100 \mu\text{s}$ or less are believed to be feasible, which may allow a significant step toward real-time beam position prediction and control.

Future work is needed in several areas to improve the applicability of this system. The prediction will need to be improved to two or more steps ahead in order to account for lag time to command the FSM. The calibration and placement of the sensors need to be refined so that submicroradian accuracy for the calculation can be achieved. Finally, the current platform sensors need to be replaced with angular rate sensors and accelerometers to more accurately model the system that would be used on a mobile platform. Once these areas are improved upon, the predicted error signal may be used with a control algorithm to position the mirror in anticipation of platform motion, allowing for the correction of platform-induced jitter at the target.

6. Acknowledgments

The authors wish to thank Directed Energy Program Manager Quentin Saulter and the Office of Naval Research for providing funding for this research. The authors also wish to thank the reviewers of this paper for their insightful and helpful comments.

References

- ¹Beggs, J.S., *J. Opt. Soc. Am.* **50**(4), 388 (1960).
- ²DeBruin, J.C., and D.B. Johnson, *Proc. SPIE* **1697**, 111 (1992).
- ³Forden, G.E., *IEEE Spectrum* **34**(9), 40 (1997).
- ⁴Gevers, M., and V. Wertz, *IEEE Trans. Autom. Control* **28**(4), 465 (1983).
- ⁵Haykin, S., *Adaptive Filter Theory*, 4th ed., Prentice Hall, Upper Saddle River, NJ (2002).
- ⁶Orzechowski, P., N. Chen, S. Gibson, and Tsu-Chin Tsao, "Adaptive Control of Jitter in a Laser Beam Pointing System," American Control Conference, 2006, June 14–16, 2006.
- ⁷Royalty, J., *Proc. SPIE* **1304**, 262 (1990).
- ⁸Skormin, V.A., T.E. Busch, and M.A. Givens, "Model Reference Control of a Fast Steering Mirror of a Pointing, Acquisition and Tracking System for Laser Communications," Proceedings of the IEEE 1995 National Aerospace and Electronics Conference, 1995, NAECON 1995, vol. 2, pp. 907–913, May 22–26, 1995.
- ⁹Skormin, V.A., M.A. Tascillo, and D.J. Nicholson, "A Jitter Rejection Technique in a Satellite-Based Laser Communication System," Proceedings of the IEEE 1993 National Aerospace and Electronics Conference, 1993, NAECON 1993, vol. 2, pp. 1107–1115, May 24–28, 1993.
- ¹⁰Smith, T., *Trans. Opt. Soc.* **30**, 68 (1928).
- ¹¹Sofka, J., V.V. Nikulin, V.A. Skormin, D.H. Hughes, and D.J. Legare, *IEEE Trans. Aerosp. Electron. Syst.* **45**(1), 336 (2009).
- ¹²Wittenmark, B., *IEEE Trans. Autom. Control* **19**(6), 848 (1974).

The Authors

Dr. Oscar Barton, Jr., is a Professor in the Mechanical Engineering Department at the U.S. Naval Academy. He received his Ph.D. in mechanical engineering in 1993 from Howard University. Professor Barton's research area focuses on the mechanical response of linear elastic structures and dynamical systems. His research interests include the use of eigenderivatives in sensitivity analysis to determine the response of composite plates and approximate methods for linear eigenvalue problems. Professor Barton also holds the Master of Science in mechanical engineering and a Bachelor of Science from Tuskegee Institute.

Midshipman Matthew Roberts is currently a Midshipman First Class at the U.S. Naval Academy. He is a Trident Scholar, Bowman Scholar, and member of the Varsity Offshore Sailing Team. He will graduate in 2010 with a B.S. in aerospace engineering. He will then report to Stanford University and complete a M.S. in mechanical engineering. Following graduate school, he will begin the Navy's Nuclear Power Program on his way to becoming a submarine officer.

CDR Joe Watkins is a Permanent Military Professor (PMP) in the Mechanical Engineering Department at the U.S. Naval Academy. He was selected for the PMP program in 2000 and began work at the Naval Postgraduate School in 2001, where he studied under Distinguished Professor Brij Agrawal and Professor Young Shin. He was awarded the Ph.D. in mechanical engineering in 2004. CDR Watkins's research area was the adaptive control of optical beam jitter. CDR Watkins also holds the Master of Science in astronautical engineering, a B.S. equivalency in electrical engineering, and a B.S. in chemical engineering from Auburn University. He was a 19-year veteran of the U.S. Navy's Submarine Force

prior to beginning his doctoral program, serving on three nuclear submarines, where his last afloat tour was as Executive Officer of USS LOUISVILLE, SSN 724. He was qualified as a nuclear engineer with the Navy as well as for command at sea prior to his selection as a PMP.